Journal of Scientific Exploration, Vol. 28, No. 3, pp. 453–476, 2014 0892-3310/14

RESEARCH ARTICLE

An Investigation of Solar Features, Test Environment, and Gender Related to Consciousness-Correlated Deviations in a Random Physical System

Joey M. Caswell
Consciousness Research Laboratory, Behavioural Neuroscience, Human Development, Laurentian University

Lyndon M. Juden-Kelly
Consciousness Research Laboratory, Behavioural Neuroscience, Human Development, Laurentian University

David A. E. Vares
Consciousness Research Laboratory, Behavioural Neuroscience, Experimental Psychology, Laurentian University

Michael A. Persinger
Consciousness Research Laboratory, Behavioural Neuroscience, Human Development, Experimental Psychology, and Biomolecular Science Programs, Laurentian University, Sudbury, Ontario, Canada
mpersinger@laurentian.ca

Submitted 3/2/2014; Accepted 5/16/2014; Published 9/30/2014

Abstract—Whereas a multitude of solar and geomagnetic variables were not correlated with significant deviations in continuous measurements from random physical systems (Random Event Generators), these variables were moderately correlated with REG output during periods of intention. The scalar components (2–10 nT) of the Interplanetary Magnetic Field (r = ~0.50) and global geomagnetic activity (r = ~0.55) were significantly correlated with REG deviations during the second minute of intention. Significance compared with nonsuccessful deviations occurred during periods of intention when the Solar Radio Flux was about 20 units ($2 \cdot 10^{-21}$ $W \cdot m^{-2}$ Hz^{-1}) higher. The polarity of the deviation was different within a Faraday (echoic) chamber than in a normal environment as well as between genders. The amount of energy associated with the increase in geomagnetic activity within the volume of human cerebrum is remarkably similar to the gravitational energy within this mass because of minute variations in G (the Gravitational Constant). These results indicate that a subset of variance shared across several components of the ambient heliogeophysical environment may be a significant mediator of intention-coupled changes in random variations in p-n junction devices, and those discrete energies associated with intrinsic variations in G may be relevant.

Introduction

The integration of biological sciences and the study of space weather were largely initiated by the original and insightful work of the biophysicist

Alexander Chizhevsky, who examined relationships between these areas within the interdisciplinary framework of heliobiology. His investigations into the effects of solar activity on terrestrial systems were wide-ranging and included human health and epidemiology, psychological well-being, electrical systems, and the behavior of entire societies (Chizhevsky 1936). Many of these correlations were supported, rediscovered, or advanced through later research using both historiometry and laboratory experiments (e.g., Persinger 1999, Halberg, Cornelissen, Otsuka, Katinas, & Schwartzkopff 2001, Gumarova, Lissen, Hillman, & Halberg 2012). Solar activity has been shown to relate to both organic and other physical systems and has potential implications for the little-understood area of anomalous cognition and apparently nonlocal physical interactions involving human consciousness.

The sun, a main-sequence star at the center of our solar system, affects the entire heliosphere, including local planetary conditions on Earth. There are a number of specific measurements associated with various types of solar activity. One particular measure is the sunspot number. Sunspots are seemingly isolated regions of the sun created by powerful magnetic activity within the solar photosphere, observations of which have been recorded since before the Common Era (Schove 1955). One reason for examining this phenomenon in the context of solar radiation is that many coronal mass ejections (CMEs) originate from areas surrounding sunspots (e.g., Hundhausen, Sawyer, House, Illing, & Wagner 1984).

One measure of sunspots is the Wolf number (R). This is a daily value used to denote the number of sunspots observed in a given day, and has been in use since 1848 (Clette et al. 2007). The formula used to obtain R is $k(10g + s)$, where k = the personal reduction coefficient, g = number of sunspot groups, and s = number of sunspots (Herrman 2012). Another measure associated with overall solar activity is the solar radio flux. This refers to radio emissions often produced when plasma within highly active regions of the sun becomes trapped beneath magnetic fields (Donnelly, Heath, Lean, & Rottman 1983), and as such are also related to sunspots. Significant correlations have been observed between daily values for these measures of solar activity (rs = ~0.6 to 0.7).

These emissions are measured at about 2,800 MHz at the 10.7-cm wavelength (Tapping 1987). The background x-ray flux is a similar measure often used, which is also related to the occurrence of solar flares (e.g., Neupert 1968, Sheeley, Howard, Koomen, & Michels 1983). Emissions in the x-ray wavelength are measured as background flux within the ionosphere (e.g., Thomson, Rodger, & Dowden 2004). This variable is typically denoted in coefficients of flux ($W \cdot m^{-2}$) ranging from low background ($<10^{-8}$) to extreme flares ($>10^{-3}$) (Thompson 2013).

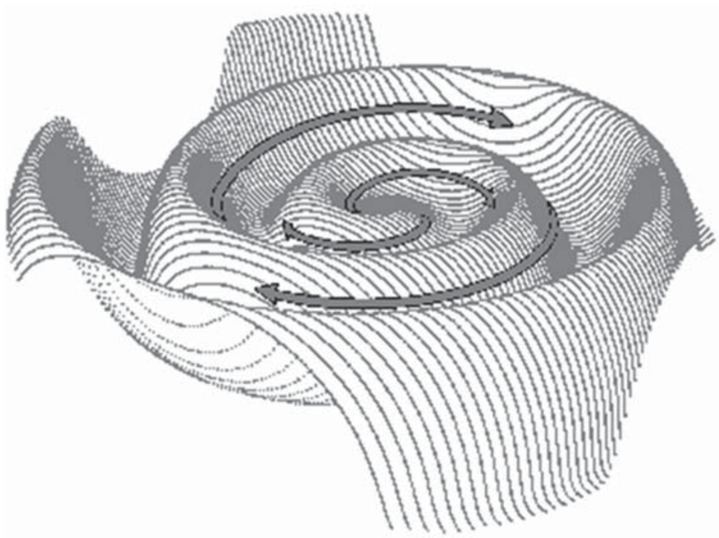

Figure 1. Representation of a "Parker spiral." Image source: NASA Cosmicopia (helios.gsfc.nasa.gov/solarmag.html)

Aside from measures directly associated with overall solar activity, there are also a number of solar wind features that are often examined in the context of space weather. The heliosphere itself is a direct product of the solar winds that pervade the solar system (Holzer 1989). This phenomenon is actually a result of particle streams released from the sun's atmosphere, and largely consists of charged electrons and protons (McComas et al. 1998). Solar proton events, or proton storms, refer to large numbers of these particles being released from the sun, and are usually associated with solar flares or CMEs (Kahler, Hildner, & Van Hollebeke 1978). These particles can enter the local magnetosphere and release their energy within the ionosphere through the process of ionization (Shea & Smart 1990).

The phenomenon of solar wind is also responsible for the interplanetary magnetic field (IMF). This refers to the magnetic field of the sun, which has been distributed among the planets of the heliosphere (Levine, Altschuler, & Harvey 1977). Because solar winds are a plasma, they have sufficient electrical conductivity—produced by a magnetohydrodynamic effect with both electric and magnetic components—to carry magnetic field lines from the sun throughout the solar system (e.g., Pogorelov, Zank, & Ogino 2004). However, as the solar magnetic field extends into interplanetary space, the sun continues to rotate on its axis, while the forces of plasma and magnetic pressure oppose one another. As a consequence of these two factors, the

IMF forms a "Parker spiral" and produces local variations throughout the heliosphere (Figure 1; Thomas & Smith 1980). This field affects not only the outer planets, but also the magnetic field of our own planet (e.g., Friis-Christensen et al. 1972).

The phenomenon of significant deviations in random systems associated with cognitive "intention" has been noted in a number of experiments. Apparently nonlocal interactions between human "intention" and non-deterministic external systems have been observed in many laboratories (e.g., Jahn, Dunne, Nelson, Dobyns, & Bradish 1997, Radin & Nelson 2003). Previous research also suggests that neurophysiological effects may mediate this apparent phenomenon of consciousness-correlated collapse (3C) or presumably random motions. This term, 3C, is preferred to traditional and now pejorative terms concerning "mind–matter" relationships. For example, electroencephalograph (EEG) activity in the alpha and beta frequencies has been shown to widen during control measures compared with periods when participants successfully achieved significant deviations in a random event generator (REG) device (Giroldini 1991). Furthermore, a relationship has been identified between the effects of cognitive "intention" and cerebral biophoton emission (Dotta & Persinger 2011, Caswell, Dotta, & Persinger 2014a) and both gravitational and electromagnetic mediated effects on the cerebral volume (Caswell, Collins, Vares, Juden-Kelly, & Persinger 2013).

Given that solar activity has been implicated as a potential factor that may affect human physiology (e.g., Cherry 2002), it was hypothesized that more subtle effects of the environment on statistically significant deviations in a random physical system correlated with consciousness may be found with factors external to the immediate geosphere. If variations of solar activity exert an influence on neurophysiological functioning, and cerebral effects are involved in the process of the 3C phenomenon, then relationships between this form of nonlocal interaction and solar variable measures should be observed. Furthermore, it was hypothesized that some form of seasonal variation in successful REG operation associated with the position of the Earth relative to the sun would be revealed.

The obvious variable of participant gender has been previously examined in the context of 3C phenomena, specifically with apparent nonlocal human–machine interactions. However, results are relatively conflicting depending on the study. This ranges from overall performance gender differences (Gissurarson 1992), differences between genders within specific modes of target data analysis (Dunne 1998), and no apparent gender differences (Nelson, Jahn, Dobyns, & Dunne 2000). Because of this disparity, it was hypothesized that there might be an environmental covariate that may mediate any 3C performance differences between males and females.

Figure 2. Random event generator (REG); A Psyleron REG-1 device used throughout the following experiments.

Methods

Subjects

Participant age ranged from 22 to 52 years for N = 26 (N = 13 females, N = 13 males). All were recruited from the Laurentian University campus or the immediate community.

Data and Equipment

Daily average values were obtained from the Goddard Space Flight Center (GSFC)/Space Physics Data Facility (SPDF) OMNIWeb interface (omniweb.gsfc.nasa.gov) for the scalar component of the interplanetary magnetic field (IMF; nT) and proton density of solar winds ($N \cdot cm^{-3}$). Daily sunspot number (R; Wolf numbers), average daily background x-ray flux (peak flux in coefficients of 10^{-6} $W \cdot m^{-2}$), and average daily solar radio flux (SFU; 1 = 10^{-22} $W \cdot m^{-2} \cdot Hz^{-1}$) were obtained from the National Oceanic and Atmospheric Administration (NOAA)/National Geophysical Data Center (NGDC) database (www.ngdc.noaa.gov). Values for the equation of time (apparent solar time) were calculated using the Local Sidereal

Time Clock maintained by Jürgen Giesen (www.jgiesen.de/astro/astroJS/siderealClock/). Finally, cosmic ray data (average impulses/min/day) was obtained from the Moscow Neutron Monitor (cr0.izmiran.rssi.ru/mosc/main.htm).

Random data was produced using a Psyleron REG-1 random event generator (Figure 2; www.psyleron.com). The device produced a random output that was generated by electron tunneling effects within two field effect transistors. The varying voltage levels that result from this process were converted into digital data through a gated sampling procedure, which allowed for regularly spaced bit sequences. The output of both transistors was internally compared through an alternating (0, 1) XOR masking process in order to reduce the potential influence of physical artifacts or other external environmental variables. The device itself was further protected from static electromagnetic factors by an aluminum outer shielding and a Permalloy mu-metal inner shield.

The device was rigorously calibrated prior to shipment to ensure that the output conformed to statistical expectations. The random event generator (REG) was also tested in control experiments within our laboratory to confirm these expectations. The resulting data were collected through a USB port using Psyleron FieldREG and Reflector software packages on a laptop computer. Data were produced at a rate of either 1 or 2 events (200 0,1 bits/event) per second (experiment-dependent), with each event referring to the number of 1's out of 200 bits with binary probabilities, represented by a value of 0 to 200. The theoretical (chance) mean for each event is 100, with a standard deviation of $\sqrt{50}$. Pilot testing and the following experiment indicated no significant differences between event rates ($p > .05$). Measures of entropy (HX) were obtained using Matlab 2011a software. All other statistical procedures were conducted using SPSS software v.17.

Procedure

In each experiment, participants were seated in a dark, comfortable environment approximately 1 m from the REG device and asked to intend for the data output to deviate either up or down (positive or negative). The device was placed on the right side of each individual. For N = 8 participants, the test location was an ordinary room, where the REG was placed at shoulder height. For the other N = 18, the test location was an acoustic chamber that was also a Faraday cage. The background average resultant fields within the cage near the REG was about 20,000 nT, compared with a typical average of 47,000 nT outside of the chamber. The REG was placed at ground level approximately 45° from the plane of the forward line of sight. Prior to testing, participants viewed a short demonstration with

Figure 3. Sample of Reflector software collecting data from REG device; jagged center line is the moving cumulative deviation.

the REG software (e.g., Figure 3) in order to understand what they would be focusing their intention on. No feedback was provided during testing. REG data collection was kept hidden from the experimenter until analysis. No significant differences were identified between varying bit rates, and averages were computed accordingly. All environmental measures were obtained following testing.

Data Analyses

Random Event Generator (REG) data were obtained from N = 26 participants within two separate experiments. Individual event scores were standardized according to .5 chance expectations ($[x - 100] / \sqrt{50}$). One experiment contributed N = 15 sessions, each lasting approximately 5 minutes. The second experiment consisted of N = 11 participants, with data collection lasting about 8 minutes. Minute averages, absolute means, and standard deviations were computed. To maintain sample consistency for statistical analysis, the first 5 minutes of testing from each participant were used for minute averages. Overall session scores were computed using Stouffer's

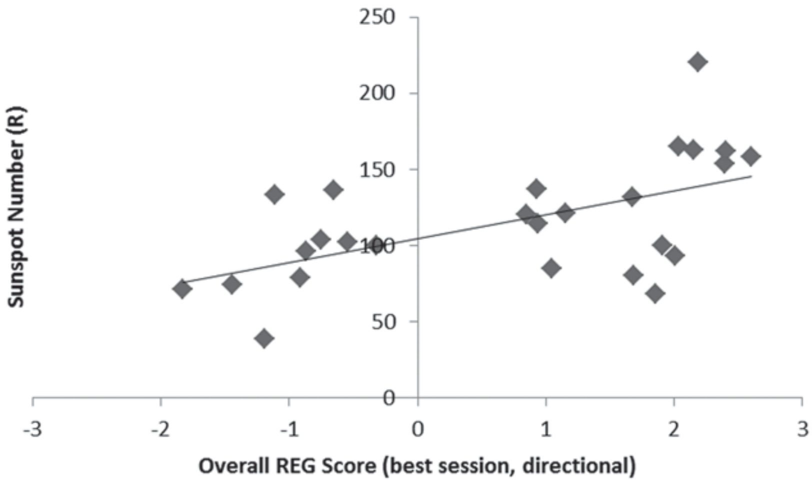

Figure 4. Correlation between sunspot number and participants' best REG score.

method ($\sum z / \sqrt{n}$), where z = individual event z-scores and n = the number of events. Various planetary and solar variables were entered into the database. Significant ($p < .05$) correlations of $r \geq .5$ were reported.

Results

REG Output without Intention

Daily averaged REG output was gathered for a period of two months. All space weather variables of interest were entered into the database and examined for potential correlations. Subsequent analyses revealed no apparent relationships between the output of a random event generator (REG) and various measures of space weather ($p > .05$). It is therefore hypothesized that any potential correlations revealed could potentially be attributed to relationships between space weather and biological/physical processes involved in the consciousness-correlated collapse (3C) of an external random process.

Solar Activity and REG Operation

Pearson and Spearman correlations revealed a statistically significant relationship between the best overall REG session score from each participant (e.g., greatest overall deviation obtained), taking direction into

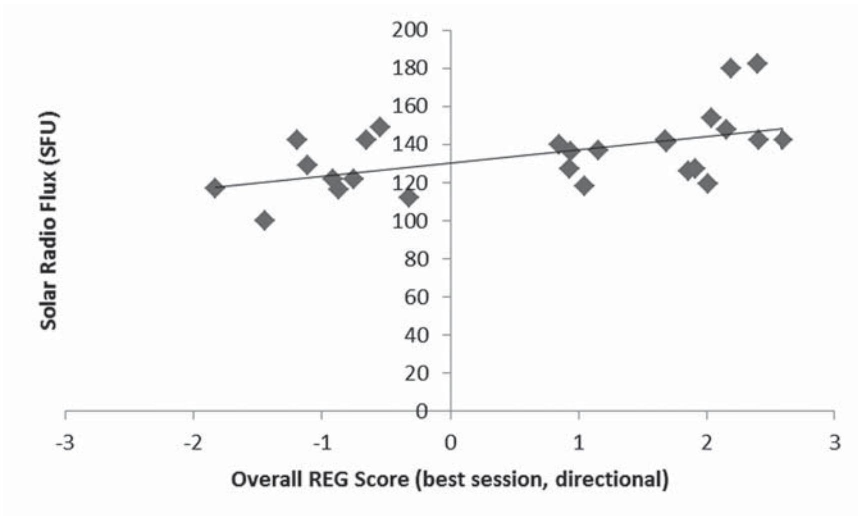

Figure 5. Correlation between solar radio flux and participants' best REG score.

account (e.g., positive value = deviation in intended direction), and both sunspot number (Figure 4; $r = .57$, $p = .002$; $rho = .601$, $p = .001$) and solar radio flux (Figure 5; $r = .541$, $p = .004$; $rho = .558$, $p = .003$). Subsequent partial correlations showed that both solar variables related to REG score independently. Their correlations vanished ($p > .05$) when controlling for the effects of the other. This suggests they shared the same source of variance with respect to the REG data.

Given the directional REG measures employed in the previous correlations (e.g., accounting for direction of intention), it appears that overall solar activity may be associated with a greater tendency for deviations correlated with operator intention. To further pursue this hypothesis, participants were split into groups determined by whether or not they had successfully achieved at least one significant REG score at the $p \leq .025$ level ($z \leq 1.96$, one-tailed; N = 8 successful, N = 18 non-successful). Independent t-tests revealed a significant difference in both sunspot number (Figure 6; $t_{(24)} = 3.865$, $p = .001$, $r = .619$) and average solar radio flux (Figure 7; $t_{(24)} = 2.924$, $p = .007$, $r = .513$) on the day of testing between successful and nonsuccessful operators (Table 1). A significant difference was also found for the average background x-ray flux (Figure 8; $t_{(24)} = 2.885$, $p = .008$, $r = .507$).

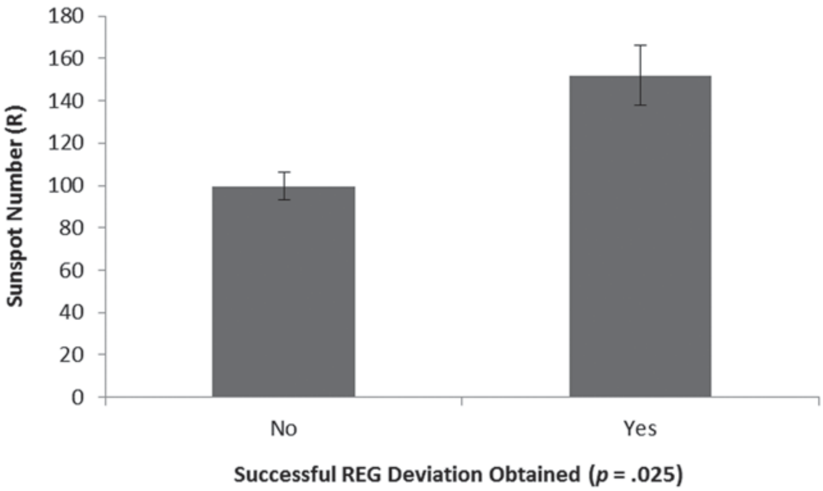

Figure 6. Difference in daily sunspot number between successful and non-successful REG operators; vertical bars represent standard error of the mean (SEM).

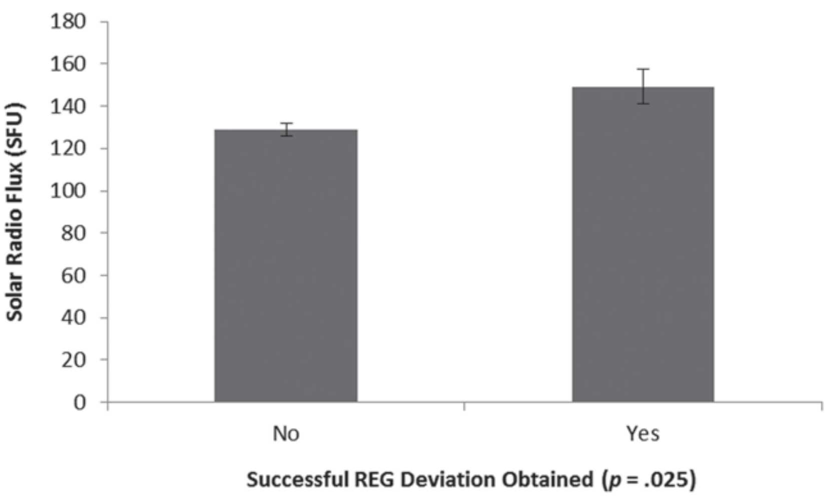

Figure 7. Difference in daily solar radio flux between successful and non-successful REG operators; vertical bars represent SEM.

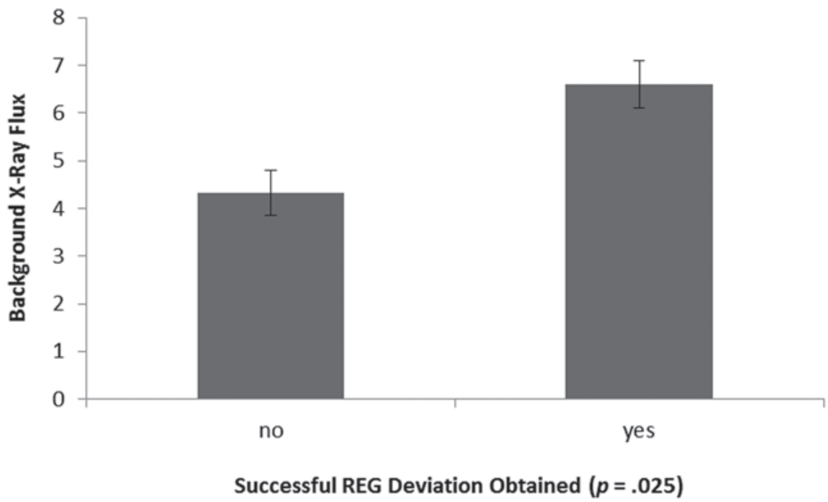

Figure 8. Difference in average daily background x-ray flux between successful and non-successful REG operators; vertical bars represent SEM.

TABLE 1
Mean (μ) and Standard Deviation (sd) Values of Sunspot Numbers, Solar Radio Flux, and Solar X-Ray Flux for Each Operator Group

REG Score	Sunspot # - μ (sd)	Radio flux - μ (sd)	X-ray flux - μ (sd)
Significant	151.88	149.25	6.60
	(40.07)	(22.54)	(1.41)
Non-significant	99.50	128.78	4.32
	(27.84)	(13.19)	(2.01)

Interplanetary Magnetic Field Correlations

Minute-to-minute averages and standard deviations were examined for potential correlations with measures of space weather, employing both parametric and nonparametric testing. A statistically significant relationship was found between average REG scores during minute 2 of testing and the scalar component of the IMF (Figure 9; $r = .51$, $p = .008$; $rho = .483$, $p = .013$). This relationship was slightly increased when controlling for the variance associated with cosmic ray impulses ($r = .526$, $p = .007$; $rho = .513$, $p = .007$). Average REG score (minute 2) and scalar IMF measures were

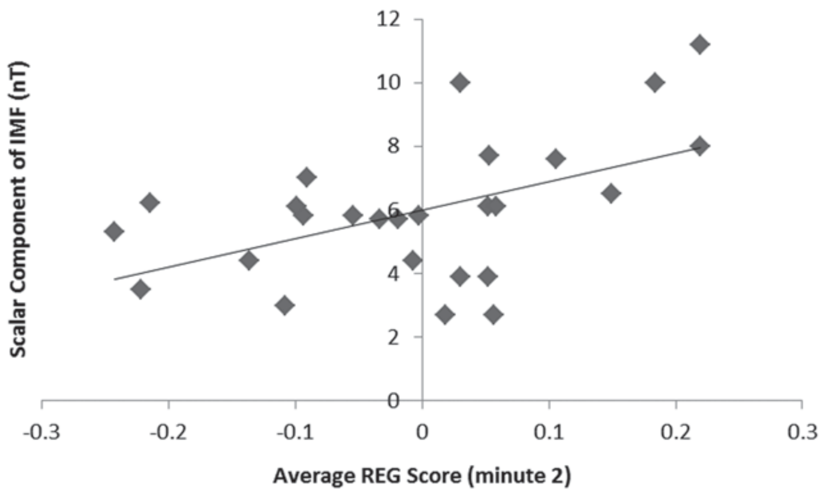

Figure 9. Correlation between the scalar IMF component and average REG score during minute 2.

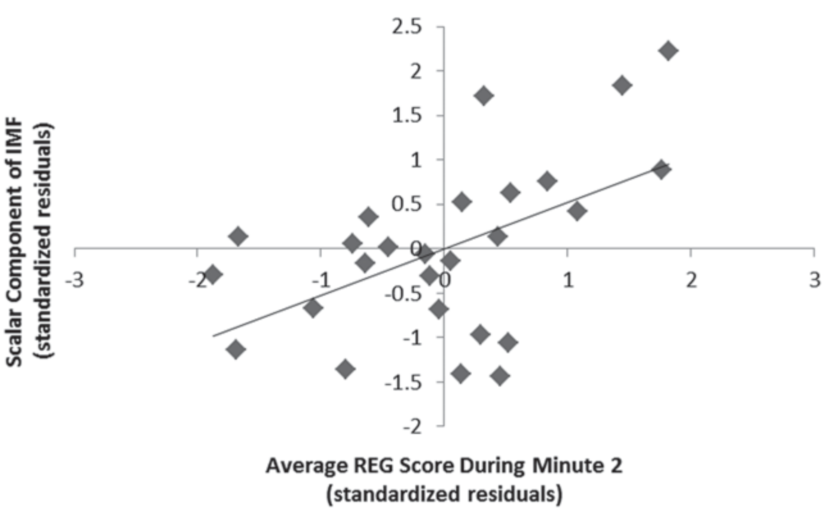

Figure 10. Partial correlation between the scalar IMF component and average REG score during minute 2, controlling for effects of cosmic ray impulses.

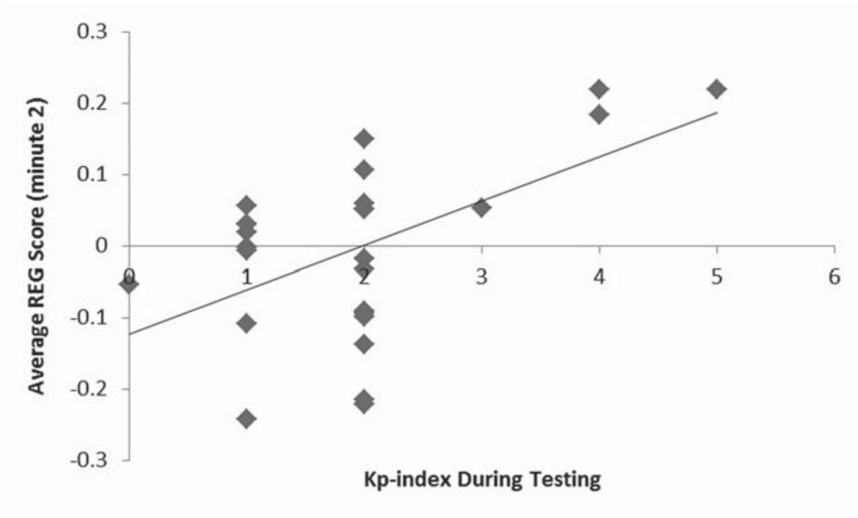

Figure 11. Averaged deviation from random (vertical axis) during the second minute of testing and the global geomagnetic index during that period.

each entered into separate linear regressions with daily averages of cosmic ray impulses as the independent variable. The subsequent standardized residuals were obtained. The partial correlation is shown in Figure 10. We previously found that this temporal component (2 minutes) appears to be particularly critical with regard to apparent human–REG interaction (Caswell, Collins, Vares, Juden-Kelly, & Persinger 2013, Caswell, Dotta, & Persinger 2014a).

Ambient Geomagnetic Conditions

The systematic correlations of similar magnitudes between REG scores and numbers of sunspots, solar flux unit output, and interplanetary magnetic field strengths indicated the association with a locality would require some representation of these changes in the vicinity of the measurements. The most obvious local representation would be global geomagnetic activity. Consequently, the daily A_p indices as well as the three-hour K_p values for the interval of the experiment and each of the three-hour increments before and after the increment were obtained from the Solen online database (www.solen.info/solar/). There was a significant correlation ($r = 0.54$, $p < .01$; *rho* $= 0.41$, $p < .05$) between the global geomagnetic activity at the time of the intention experiments and the REG deviations. These results are shown in Figure 11.

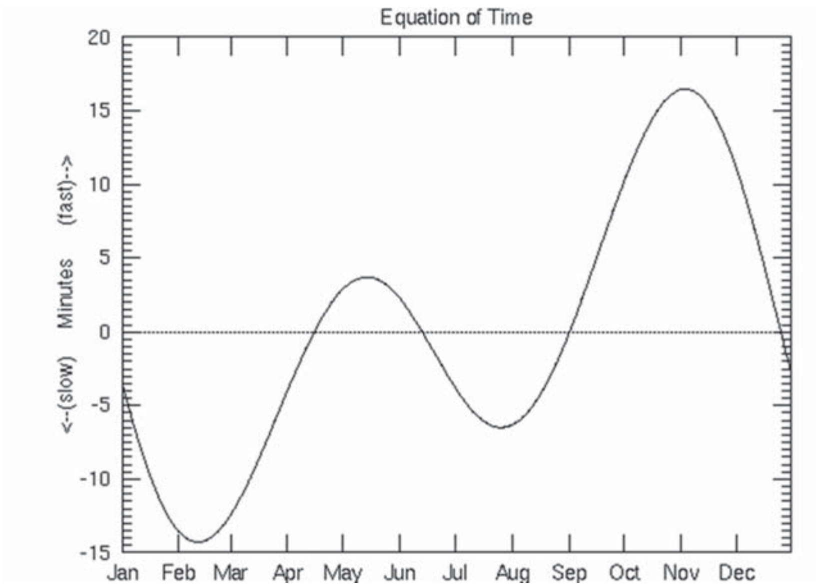

Figure 12. Equation of time; difference between mean solar time and apparent solar time throughout the year. Image source: Nick Strobel (www.astronomynotes.com/nakedeye/s9.htm)

Isolating Shared Sources of Variance

To discern the potential sources of shared variance, a factor analysis was completed for the magnitude of the REG variation during the second minute, sunspot numbers for the day, IMF values for the day, solar flux units for the day, and the K_p indices (ambient, but global geomagnetic activity) for the interval in which the measurements were obtained. To accommodate the small sample size, loading coefficients of >0.70 were considered significant. The first factor (eigenvalue = 2.38), which accommodated almost half of the variance, was loaded significantly by the K_p values (0.85), IMF (0.85), and the REG variation during the second minute (0.83). The second factor (eigenvalue = 1.53), which explained 31% of the variance, was loaded significantly by numbers of daily sunspots and solar flux units. Together the two factors accommodated 78% of the variance. These results indicate that the proximal geophysical (interplanetary magnetic field and geomagnetic field variations) variables share a source of variance with the REG variations.

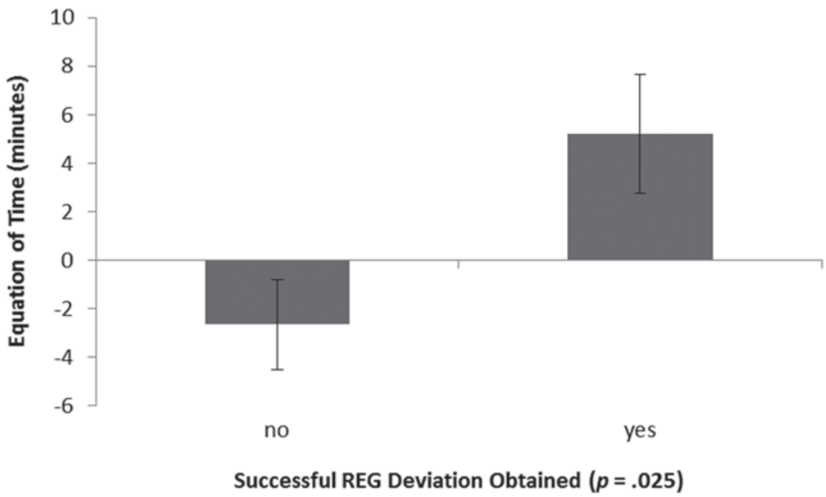

Figure 13. Difference in equation of time (minutes) between successful and nonsuccessful REG operators; vertical bars represent SEM.

Time and REG Performance

Although standard time measures noon with regard to the position of the sun relative to the local meridian, the actual time of this crossing varies throughout the year. The equation of time represents the difference between mean solar time and apparent solar time. The difference between these two times varies by up to 16 minutes in either direction (Figure 12). Values for the equation of time (in minutes) were obtained from an online Sidereal Time calculator for each test session (Table 2). Values for the equation of time can be approximated using (GAST – α) – (UT + Offset), where GAST = Greenwich apparent sidereal time, α = right ascension of apparent Sun, and UT = Universal Time. Independent t-test analysis determined that there was a significant difference in the values associated with the equation of time and the occurrence of REG session scores of $p \leq .025$ (Figure 13; $t_{(24)} = 2.429$, $p = .023$, $r = .444$). This may suggest some form of seasonal variation associated with the occurrence of various "psi" processes, which may also provide an explanation for why some experiments have been unsuccessful in the past.

TABLE 2
Mean (μ) and Standard Deviation (sd) Values for the Equation of Time Values (in Minutes) between REG Operator Groups

Equ (min)	Significant	Non-Significant
μ	5.219	−2.648
Sd	(6.909)	(7.897)

Test Location and REG Outcome

Finally, N = 8 participants completed testing within a normal room, while N = 18 were tested within an acoustic chamber that was also a Faraday cage. Initially, there were no indications of significantly different REG session scores between locations. However, when entered into an analysis of covariance (ANCOVA), a significant difference was found for the best session score (e.g., greatest deviation obtained) between locations when covarying for the solar wind proton density ($F_{(1, 25)} = 4.808$, $p = .039$, $\eta^2 = .162$). A linear regression was run for REG scores with proton

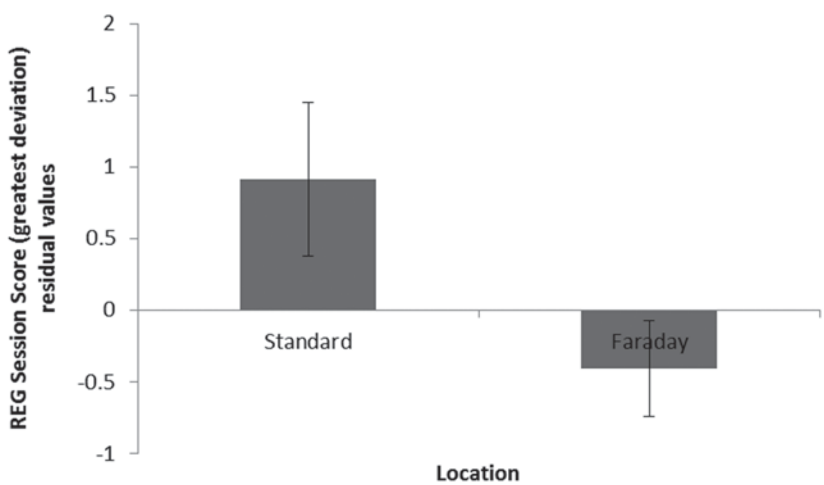

Figure 14. Difference in best REG session score obtained between locations, covarying for solar wind proton density; vertical bars represent SEM.

TABLE 3
Mean (μ) and Standard Deviation (sd) Values of REG Session Entropy (HX) for Male and Female Participants

HX (REG)	Female	Male
μ	2.37	2.27
Sd	(.068)	(.121)

density as the independent variable to obtain standardized residuals for demonstrating this significant difference in Figure 14. More specifically, more positive deviations occurred within the standard location ($\mu = .578$, $sd = .955$), while more negative deviations were obtained within the Faraday cage ($\mu = -.257$, $sd = .9$).

Gender, REG Performance, and Complexity

Signal complexity of the REG event data for each session was obtained using the entropy function in Matlab software. The measure of entropy computed by this method is similar to the Shannon entropy of a random variable (e.g., Shannon 1948), $H(X) = -\sum_x P(x)\log_2 P(x)$, where x = the random variable,

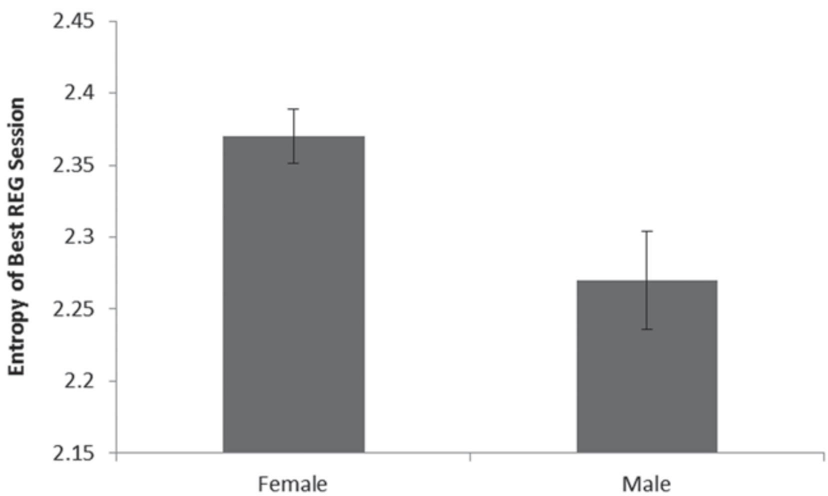

Figure 15. Entropy (HX) values of REG data (greatest deviation) for males and females.

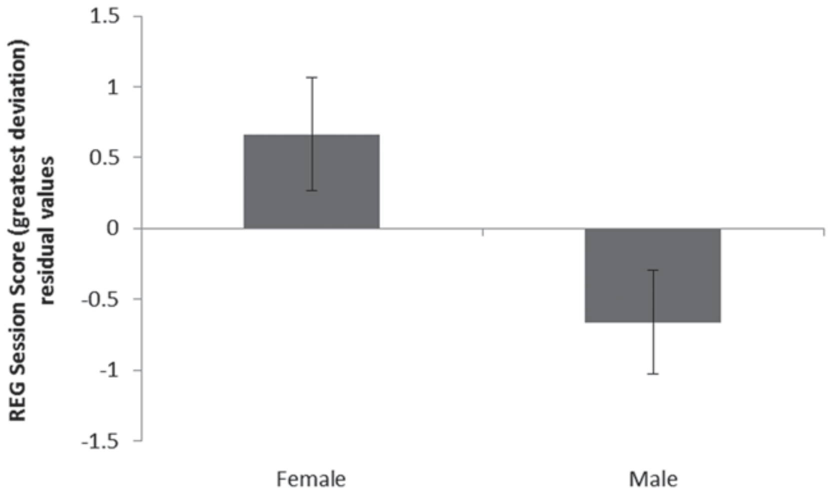

Figure 16. Difference in overall REG score (best session for each participant) between genders, controlling for the effects of lunar apogee/ perigee; vertical bars represent SEM.

X = the number of possible values within x, and P = the probability mass function. Entropy values (HX) represent the level of uncertainty within the data, where higher values indicate greater complexity and less predictability. Signals with greater complexity possess a greater number of distinct values, and these values are more evenly distributed. Using an independent t-test, it was determined that HX values of each participant's best REG session (greatest deviation) were significantly greater for females than males (Figure 15 and Table 3; $t_{(24)} = 2.523$, $p = .019$, $r = .454$).

Given the relationship between the reproductive cycle with associated hormonal changes and the lunar cycle (e.g., Cutler, Schleidt, Friedmann, Preti, & Stine 1987), it was hypothesized that if there were further differences between genders with regard to REG operation, the relative position of the moon may be a factor. Subsequently, an ANCOVA was used to compare REG deviations between males and females while covarying for the effects of both lunar apogee and perigee. Distance from the moon was measured by the number of days since the most recent lunar apogee and perigee for each session, as derived from the Lunar Extremes database. The greatest REG session score obtained by each participant (e.g., largest overall deviations) differed significantly between genders, with the greatest effect found when simultaneously controlling for both apogee and perigee (Figure 16; $F_{(1, 25)} = 5.802$, $p = .025$, $\eta^2 = .186$). More specifically, females obtained significantly more positive (μ = .42, *sd* = .912) scores, while male operators resulted in more negative scores (μ = −.42, *sd* = .232).

Discussion

We measured moderately strong correlations between solar and geomagnetic variables and the deviation from chance from electronic outputs from random event generators when people were intending to alter these outputs. On the other hand, there were no significant correlations between these variables and the output of the REG when there were no subjects in proximity. These results suggest that an interaction between solar–geomagnetic variables, some physical aspect of human cognition (intent), and random variations from electron tunnelling through p-n junctions at a distance of approximately 1 m may have occurred. We cannot exclude the possibility that simply the mass or presence of the person produced these effects. However, in other experiments (Caswell, Vares, Juden-Kelly, & Persinger 2014b) involving the exposure of subjects to experimentally produced magnetic fields, intention with the presentation of those fields was required to affect the significant deviations. Periods of no-intention, even with the field present, produced changes that did not differ significantly from the no-intention, no-field condition.

Although the solar and geomagnetic variables we employed in this study are strongly intercorrelated, the energy values associated with the most specific proximity values could be revealing. The mean solar flux units (sfu) during successful REG deviations was about 140 in comparison with deviations that did not differ from chance (120). Because 1 sfu = 10^{-22} $W{\cdot}m^{-2}\ Hz^{-1}$, this means that at the level of the typical width of a p-n junction (with an average p and n width of about $0.5 \cdot 10^{-6}$ m) and the lower end of the width of a synapse ($0.5{\cdot}10^{-6}$ m), the energy at one unit time at 140 sfu (when there was significant deviation) would be $3.5{\cdot}10^{-33}$ J, while the energy at one unit time around 120 sfu would be $3.0{\cdot}10^{-33}$ J. The difference of 20 sfu between the two is equivalent to $5{\cdot}10^{-34}$ J. When divided by Planck's constant ($6.626{\cdot}10^{-34}$ J·s), this difference is the equivalent shift (increase) of frequency of about 0.5 to 1 Hz. This frequency is within the range of both dc–ac interfaces in cerebral activity as well as hydromagnetic (hm) waves produced by interactions between the geomagnetic magnetic field and variations in the interfacing interplanetary magnetic field.

If we assumed that the entire cerebrum was involved, with approximately $\sim 6{\cdot}10^{13}$ synapses, the total additional energy output from the $3.0{\cdot}10^{-33}$ J would be $\sim 3{\cdot}10^{-20}$ J per second. Although more likely to be incidental than real, if the total energy available of this magnitude were integrated per second, the possibility that the state of the entire cerebrum might be shifted by a single neuron affected by these forces becomes feasible. There is experimental evidence that the activity of a single neuron can shift the state of an entire rat's cerebral cortices (Cheng-Yu, Poo, & Dan 2009). In addition, a single neuron's state is the initiating condition for a more grossly expressed behavior, such as the display or lack of display of an operant response (Houweling & Brecht 2007), which involves millions of neurons.

The role of gravitational phenomena in REG-related deviations has often been neglected because of the assumption of low energies and minimal forces for local space and matter. However, recently Persinger and St-Pierre (2014) showed that the "random variation" in G ($6.67 \cdot 10^{-11}$ $m^3 \cdot kg^{-1} \cdot s^{-2}$), which is about 10^{-14} $m^3 \cdot kg^{-1} s^{-2}$, was moderately and negatively correlated with the strength of the interplanetary magnetic field within the range of ± 8 nT. The gravitational energy from this variation within a mass of 1 L of water (the approximate proportion of water within the volume of the human brain) would be $\sim 3 \cdot 10^{-14}$ J. On the other hand, the energy from 8 nT within the volume of 1 L of water would be $3 \cdot 10^{-14}$ J. The mass–energy equivalence for this quantum of energy is the same order of magnitude as the electron (10^{-31} kg).

Although these correlations would be consistent with a nonlocality explanation for the deviations from random exhibited by the REG, the potential local effects cannot be ignored. The correlation between REG scores and geomagnetic activity within which the subject and the equipment would have been immersed was 0.54. This would suggest that the other correlations with solar and IMF variables were significant because they were correlated with the changes in the local geomagnetic field. This inference was supported by the exploratory factor analysis (considering the small sample size) that indicated more than 70% of the variance for the REG deviations during the second minute, global geomagnetic activity at the time of the measurement, and interplanetary magnetic field variations shared a common source. On the other hand, the direct solar measurements (sunspot number and solar flux units) shared variance on a separate factor.

The actual geomagnetic intensity during the experiments was between 0 and 5. This is equivalent to variations of 0 to 2 nT and 48 to 56 nT. The greatest deviations (Figure 11) during intention occurred when the geomagnetic activity was above ~20 nT. This would have been a substantial difference in the magnetic energy stored within the cerebral volume. According to traditional formulae, the value would be $2.4 \cdot 10^{-13}$ J during the greatest deviations and $2 \cdot 10^{-15}$ J during the smallest deviations. Assuming each action potential is associated with $2 \cdot 10^{-20}$ J, the induced energy during the magnetic field oscillations would be equivalent to the discharge of 10^7 neurons. This is within the order of magnitude of the neurons associated with specific cognitions as inferred by fMRI studies. Assuming an average of 58 neurons per cubic mm, this number of total neurons (if cluster in proximity rather than distributed) could involve a volume of $1.2 \cdot 10^{-4}$ m^3, or less than 10% of the total volume.

Because the significant correlation between geomagnetic variation and REG occurred during the second minute (60 to 120 s) of this measurement, the mean power (assuming an average of 90 s or 0.01 Hz) would have been $2.4 \cdot 10^{-15}$ W. Given the typical cross-sectional area of 10^{-2} m^2, this would be equivalent to about $2.4 \cdot 10^{-13}$ W·m^{-2}. Interestingly, this value is within the range of background cosmic ray power density at the earth's surface. Cosmic (proton) ray background has been considered one source of "random variation." If the volume containing the number of estimated neurons (10^7) is considered, the volume of brain mass would extend a length of about 5 cm. With this cross-sectional area ($2.5 \cdot 10^{-3}$ m^2), the power density would be on the order of 10^{-11} W·m^{-2} to 10^{-10} W·m^{-2}. This power density is within the range of that associated with photon emission from the cerebrum during cognition (Saroka et al. 2013).

From a traditional heliogeophysical perspective, the ultimate source of the variation that produced the shifts in REG output while the person was intending originated from the sun. The results of the factor analysis indicate that the solar (distal) variables were less related than the proximal (interaction between the interplanetary magnetic field and global geomagnetic field) variables. However, there would be a physical coupling between the two sources. We suggest that a subset of energies originating from the sun and mediated through the interplanetary magnetic field (which is the sun's magnetic field) to the geomagnetic volume within which the person is immersed contributed to the REG changes. Because intention was required, one interpretation is that some component of solar-originating energies interacted with the processes associated with neurocognition.

The difference in polarity between the REG, that is positive or negative deviation, as a function of the location in which the subjects were tested may help reveal the potential source of the negative or positive drift in these studies. The "normal" room, within which positive deviations occurred, was measured after the experiment by a magnetometer that displayed these parameters: resultant field: 46,770 nT, inclination: 70.6 deg. On the other hand, these values within the Faraday cage (acoustic chamber) were 19,822 nT and 53.8 deg, respectively. The latter value is within the range of magnitude of that found along the equator where the imaginary shift in polarity between North Pole and South Pole flux lines would occur. However, because we did not test the REG in multiple sites that displayed similar intensities outside of the acoustic chamber, we cannot conclude if the direction of the REG deviation was caused by the unique location or the magnetic field discrepancy.

None of the solar–geomagnetic variables were associated with the entropy of the REG scores. The only category that displayed a statistically significant difference involved gender. This is particularly interesting when compared with differences in statistical complexity for female–male EEG measures. Ahmadi et al. (2013) examined the complexity of EEG profiles using fractal dimensions. Although this method differs from entropy, when the mean values of all EEG channels were averaged together within each gender, the ratio of female–male complexity (as determined by fractal dimension) was strikingly similar to that obtained for REG entropy measures of female–male complexity (1.02 and 1.04, respectively). The presence of male–female differences in complexity may help explain an interesting historical pattern involved with spontaneous cases of "poltergeists." The ratio of females to males ranges between 2:1 and 20:1, depending upon the study. If the gender differences in electroencephalography and complexity are applicable, then the role of space–time geometry and the information within the matter affected by the proximity of these individuals could be investigated.

Acknowledgments

The authors wish to thank Kevin S. Saroka and Nancy V. Caswell for their insightful comments and suggestions.

References

Ahmadi, K., Ahmadlou, M., Rezazade, M., Azad-Marzabadi, E., & Sajedi, F. (2013). Brain activity of women is more fractal than men. *Neuroscience Letters, 535*, 7–11.

Caswell, J. M., Collins, M. W. G., Vares, D. A. E., Juden-Kelly, L. M., & Persinger, M. A. (2013). Gravitational and experimental electromagnetic contributions to cerebral effects upon deviations from random number variations generated by electron tunneling. *International Letters of Chemistry, Physics and Astronomy, 11*, 72–85.

Caswell, J. M., Dotta, B. T., & Persinger, M. A. (2014a). Cerebral biophoton emission as a potential factor in non-local human machine interaction. Submitted.

Caswell, J. M., Vares, D. A. E., Juden-Kelly, L. M., & Persinger, M. A. (2014b). Simulated effects of sudden increases in electromagnetic activity on deviations in random electron tunneling behaviour associated with cognitive intention. Submitted.

Cheng-Yu, T. L., Poo, M. M., & Dan, Y. (2009). Burst spiking of a single cortical neuron modifies global brain state. *Science*, *324*(5927), 643–646.

Cherry, N. (2002). Schumann resonances, a plausible biophysical mechanism for the human health effects of Solar. *Natural Hazards, 26*(3), 279–331.

Chizhevsky, A. (1936). *The Terrestrial Echo of Solar Storms*. Moscow: Mysl'Press.

Clette, F., Berghmans, D., Vanlommel, P., Van der Linden, R. A. M., Koeckelenbergh, A., & Wauters, L. (2007). From the Wolf number to the International Sunspot Index: 25 years of SIDC. *Advances in Space Research, 40*(7), 919–928.

Cutler, W. B., Schleidt, W. M., Friedmann, E., Preti, G., & Stine, R. (1987). Lunar influences on the reproductive cycle in women. *Human Biology*, *59*(6).

Donnelly, R. F., Heath, D. F., Lean, J. L., & Rottman, G. J. (1983). Differences in the temporal variations of solar UV flux, 10.7-cm solar radio flux, sunspot number, and Ca-K plage data caused by solar rotation and active region evolution. *Journal of Geophysical Research: Space Physics, 88*(A12), 9883–9888.

Dotta, B. T., & Persinger, M. A. (2011). Increased photon emissions from the right but not the left hemisphere while imagining white light in the dark: The potential connection between consciousness and cerebral light. *Journal of Consciousness Exploration & Research, 2*(10), 1463–1473.

Dunne, B. J. (1998). Gender differences in human/machine anomalies. *Journal of Scientific Exploration*, *12*(1), 3–55.

Friis-Christensen, E., Lassen, K., Wilhjelm, J., Wilcox, J. M., Gonzalez, W., & Colburn, D. S. (1972). Critical component of the interplanetary magnetic field responsible for large geomagnetic effects in the polar cap. *Journal of Geophysical Research, 77*(19), 3371–3376.

Giroldini, W. (1991). Eccles's model of mind–brain interaction and psychokinesis: A preliminary study. *Journal of Scientific Exploration, 5*(2), 145–161.

Gissurarson, L. R. (1992). The psychokinesis effect: Geomagnetic influence, age and sex differences. *Journal of Scientific Exploration*, *6*(2), 157–165.

Gumarova, L., Lissen, G. C., Hillman, D., & Halberg, F. (2012). Geographically selective assortment of cycles in pandemics: Meta-analysis of data collected by Chizhevsky. *America, 12*, 15.

Halberg, F., Cornelissen, G., Otsuka, K., Katinas, G., & Schwartzkopff, O. (2001). Essays on chronomics spawned by transdisciplinary chronobiology. *Neuroendocrinology Letters, 22*(5), 359–384.

Herrman, P. L. (2012). Glossary of terms for the data available in the N0NBH solar banners. http://www.hamqsl.com/Glossary.pdf

Holzer, T. E. (1989). Interaction between the solar wind and the interstellar medium. *Annual Review of Astronomy & Astrophysics, 27*, 199–234.

Houweling, A. R., & Brecht, M. (2007). Behavioural report of single neuron stimulation in somatosensory cortex. *Nature, 451*(7174), 65–68.

Hundhausen, A. J., Sawyer, C. B., House, L., Illing, R. M. E., & Wagner, W. J. (1984). Coronal mass ejections observed during the Solar Maximum Mission: Latitude distribution and rate of occurrence. *Journal of Geophysical Research: Space Physics, 89*(A5), 2639–2646.

Jahn, R. G., Dunne, B. J., Nelson, R. D., Dobyns, Y. H., & Bradish, G. J. (1997). Correlations of random binary sequences with pre-stated operator intention: A review of a 12-year program. *Journal of Scientific Exploration, 11*(3), 345–367.

Kahler, S. W., Hildner, E., & Van Hollebeke, M. A. I. (1978). Prompt solar proton events and coronal mass ejections. *Solar Physics, 57*(2), 429–443.

Levine, R. H., Altschuler, M. D., & Harvey, J. W. (1977). Solar sources of the interplanetary magnetic field and solar wind. *Journal of Geophysical Research, 82*(7), 1061–1065.

McComas, D. J., Bame, S. J., Barker, P., Feldman, W. C., Phillips, J. L., Riley, P., & Griffee, J. W. (1998). Solar wind electron proton alpha monitor (SWEPAM) for the Advanced Composition Explorer. In C. Russell, R. Mewaldt, & T. Von Rosenvinge (Editors), *The Advanced Composition Explorer Mission* (pp. 563–612). Netherlands: Springer Netherlands.

Nelson, R. D., Jahn, R. G., Dobyns, Y. H., & Dunne, B. J. (2000). Contributions to variance in REG experiments: ANOVA models and specialized subsidiary analyses. *Journal of Scientific Exploration*, *14*(1), 73–89.

Neupert, W. M. (1968). Comparison of solar x-ray line emission with microwave emission during flares. *The Astrophysical Journal, 153*, 59–64.

Persinger, M. A. (1999). Wars and increased solar-geomagnetic activity: Aggression or change in intraspecies dominance? *Perceptual and Motor Skills, 88*, 1351–1355.

Persinger, M. A., & St-Pierre, L. (2014). Is there a geomagnetic component to variation in G? Submitted.

Pogorelov, N. V., Zank, G. P., & Ogino, T. (2004). Three-dimensional features of the outer heliosphere due to coupling between the interstellar and interplanetary magnetic fields: I. Magnetohydrodynamic model: Interstellar Perspective. *The Astrophysical Journal, 614*(2), 1007.

Radin, D. I., & Nelson, R. D. (2003). Meta-analysis of mind-matter interaction experiments: 1959–2000. In *Healing, Intention, and Energy Medicine* (pp. 39–48). London: Harcourt Health Sciences.

Saroka, K. S., Dotta, B. T., & Persinger, M. A. (2013). Concurrent photon emission, changes in quantitative brain activity over the right hemisphere, and alterations in the proximal geomagnetic field while imagining white light. *International Journal of Neuroscience, 3*(1), 30–34.

Schove, D. J. (1955). The sunspot cycle, 649 BC to AD 2000. *Journal of Geophysical Research, 60*(2), 127–146.

Shannon, C. E. (1948). A mathematical theory of communication. *The Bell System Technical Journal*, *27*, 379–423, 623–656.

Shea, M. A., & Smart, D. F. (1990). A summary of major solar proton events. *Solar Physics, 127*(2), 297–320.

Sheeley, N. R., Howard, R. A., Koomen, M. J., & Michels, D. J. (1983). Associations between coronal mass ejections and soft x-ray events. *The Astrophysical Journal, 272*, 349–354.

Tapping, K. F. (1987). Recent solar radio astronomy at centimeter wavelengths: The temporal variability of the 10.7-cm flux. *Journal of Geophysical Research: Atmospheres, 92*(D1), 829–838.

Thomas, B. T., & Smith, E. J. (1980). The Parker spiral configuration of the interplanetary magnetic field between 1 and 8.5 AU. *Journal of Geophysical Research: Space Physics, 85*(A12), 6861–6867.

Thompson, R. (2013). Meaning of x-ray fluxes from the sun. http://www.ips.gov.au/Educational/2/1/3

Thomson, N. R., Rodger, C. J., & Dowden, R. L. (2004). Ionosphere gives size of greatest solar flare. *Geophysical Research Letters, 31*(6).